Review

Ultrasmall-in-Nano Approach: Enabling the Translation of Metal Nanomaterials to Clinics

Domenico Cassano, Salvador Pocoví-Martínez, and Valerio Voliani

Just Accepted

Ultrasmall-in-Nano Approach: Enabling the Translation of Metal Nanomaterials to Clinics

Domenico Cassano[+,†,‡], Salvador Pocoví-Martínez[+,§], and Valerio Voliani[*,†]

† Center for Nanotechnology Innovation@NEST, Istituto Italiano di Tecnologia, Piazza San Silvestro, 12 - 56126, Pisa, Italy.

‡ NEST-Scuola Normale Superiore, Piazza San Silvestro, 12 - 56126, Pisa, Italy.

§ Institute of Clinical Physiology, National Research Council, Via G. Moruzzi, 1 – 56124, Pisa, Italy

*Corresponding author: valerio.voliani@iit.it

[+]These Authors have contributed equally.

ABSTRACT: Currently, nanomaterials are of widespread use in daily commercial products. However, the most promising and potentially impacting application is in the medical field. In particular, nano-sized noble metals hold the promise to shift the current medical paradigms for the detection and therapy of neoplasms thanks to the: i) localized surface plasmon resonances (LSPRs), ii) high electron density, and iii) suitability for straightforward development of all-in-one nano-platforms. Nonetheless, there is still no clinically approved noble metal nanomaterial for cancer therapy/diagnostic. The clinical translation of noble metal nanoparticles (NPs) is mainly prevented by the issue of persistence in organism after the medical action. Such persistence increases the likelihood of toxicity and the interference with common medical diagnoses. Size-reduction to ultrasmall nanoparticles (USNPs) is a suitable approach to promote metal excretion by the renal pathway. However, most of the functionalities of NPs are lost or severely altered in USNPs, jeopardizing clinical applications. A groundbreaking advance to jointly combine the appealing behaviors of NPs with metal excretion relies on the ultrasmall-in-nano approach for the design of all-in-one degradable nano-platforms comprising USNPs. Such nano-architectures might lead to the delivery of a novel paradigm for nanotechnology, enabling the translation of noble metal nanomaterials to clinics in order to treat carcinomas in a less invasive and more efficient manner. This review covers the recent progresses related to this exciting approach. The most significant nano-architectures designed with the ultrasmall-in-nano approach are discussed, and their perspectives provided.

INTRODUCTION

The first medical nanosystems for the treatment of solid neoplasms were introduced to the market in the late 20th century.[1] The main aims of these early nanomaterials were to improve diagnosis accuracy and to increase the efficacy of known but poorly bioavailable drugs.[2] Nowadays, research on nanomaterials is aimed at improving early diagnosis of neoplasms, as well as at decreasing the side-effects of therapies while increasing their action. The overarching goal of research in this field is to unlock novel combined treatments, due to the unique physical, chemical and physiological features of the matter at the nanoscale.[3]

A number of key features, among which size, payload density, combination of different moieties, surface decoration, and intrinsic behaviors make nanomaterials promising candidates for cancer applications with enhanced potential efficacy with respect to small molecules.[3,4] For example, the pharmacokinetic profile of nanoparticle-incorporated drugs often includes a dramatic increase in circulation half-life ($t_{1/2}$) compared to the drug alone, together with a significant increase in accumulation within the target.[3] On this hand, Doxil®, a PEGylated liposome loaded with doxorubicin, exhibits a 100-times increased circulation half-life and a seven-fold lower cardiotoxicity with respect to free doxorubicin.[5] Furthermore, nanomaterials are appealing for combining diagnostics and therapeutics moieties on the same platform (*i.e.*, theranostics).[5,6] Theranostic agents can simultaneously deliver imaging and therapeutic agents to specific sites or organs, enabling detection and treatment of diseases in a single

1

procedure and, thus, improving the patient outcome.[7,8] For instance, one of the most promising multifunctional agent is known as porphysome.[9] Porphysomes are porphyrins/phospholipids assemblies, which have been recently investigated in animal models as photothermal (PT), photodynamic (PD), ultrasound (US), positron emission tomography (PET) and photoacoustic (PA) agents, as well as drug carriers.[10,11] These tools will be able to help physicians to make informed decisions about timing, dosage, drug choice, and treatment strategies.
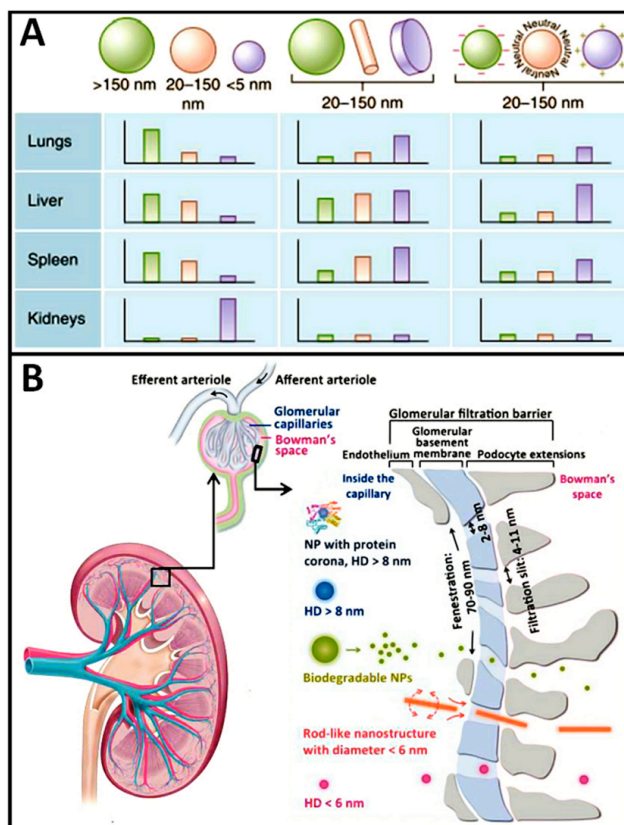

Figure 1. Panel A: *in vivo* biodistribution of nanoparticles (NPs) in healthy models is size, shape and surface charge dependent. Left) The size of both hard or soft spherical nanoparticles strongly influences the excretion of nanomaterials from organisms. When the diameter is up to hundreds of nm, NPs accumulate within lung, spleen and liver. In the size range of 20-150 nm, NPs can also accumulate in neoplasms (if present) by enhanced permeability and retention (EPR) effect. Under the threshold of 5 nm, injected nanoparticles are rapidly filtered and excreted by the kidneys.[12] Center) Due to intrinsic flow characteristics, biodistribution and pharmacokinetics of anisotropic nanomaterials are severely altered compared to spherical particles of the same size.[13] Right) Surface charge also influences biodistribution and pharmacokinetics of nanomaterials, due to different protein corona formation.[14,15] Panel B: schematic representation of a kidney and highlight of its fine microstructure. Glomerular filtration is similar to a size exclusive/gel filtration chromatography.[16,17] Panel A adapted from ref. 15 by permission from MacMillan Publishers Ltd. Panel B adapted from ref. 16 with permission from Elsevier.

Nanomaterials can be grouped accordingly to their mechanical properties, with polymers, lipid vesicles, dendrimers, and polymer-protein conjugates being at the 'soft' end of the spectrum, and inorganic materials, in particular metals, at the 'hard' one.[4,18] Within the large portfolio of nanomaterials, noble metal nanoparticles (NPs) show intrinsic multi-functionalities due to both the high electron density and the peculiar interaction with electromagnetic waves, the latter known as localized plasmon surface resonance (LSPR).[19,20] For example, gold NPs interact with ionizing radiation increasing the photoelectric emission rate, acting as both local radiation dose enhancers (enhanced radiation therapy, eRT) and contrast agents for X-ray computed tomography (CT), providing tumor boundaries demarcation. Furthermore, photon-phonon coupling afford the possibility to exploit NPs for photothermal therapy (PTT).[21,22] A number of potential applications of metal nanomaterials in medicine are comprehensively discussed elsewhere.[23–26] These behaviors make NPs ideal candidates for the design of theranostic tools which hold the great promise to shift the current medical paradigms in cancer treatment.[27,28]

To date, more than 40 nanosystems for healthcare applications are on the market.[4] The large majority of

2

1
2
3
4
5
6
7
8
9
10
11
12
13
14
15
16
17
18
19
20
21
22
23
24
25
26
27
28
29
30
31
32
33
34
35
36
37
38
39
40
41
42
43
44
45
46
47
48
49
50
51
52
53
54
55
56
57
58
59
60

these platforms are soft nanomaterials.[2,4,18] Just four inorganic nanomaterials (iron oxide) are already on the market, following the 1996 FDA-approval of Endorem® (Guerbet) for magnetic resonance imaging (MRI) diagnostics.[18] Remarkably, there is still no approved noble metal nanomaterial for cancer therapy.[2,4,18] The only approved platform using gold nanospheres is a tool for bench diagnostics called Verigene®.[2] This lack of translation is mainly related to the concern of NPs persistence in organisms after the designed action, confining all their intriguing features to the bench-side (Fig. 1-A).[15,18,29] Indeed, NPs are not biodegradable, and their conventional size as theranostic agents is over 20 nm.[18] Excretion is an essential biological process that prevents damage and toxicity by eliminating materials from organisms.[30] There are two major excretion routes: renal (urine) and hepatic (bile to feces) pathways. The renal pathway is a passive excretion route that relies on glomerular filtration in kidneys, whose efficiency is affected by the material size, charge, and shape (Fig. 1-B).[30] The size-threshold of glomerular walls is typically less than 8 nm, indicating that renal excretion is exclusive only for materials with ultrasmall hydrodynamic diameters (HDs).[6] It is important to notice here that endogenous proteins can interact with nanomaterials (protein corona formation), resulting in an increase of the HD of NPs respect to their original size.[31–33] Excretion of objects above 10 nm occurs through liver and spleen into bile and feces.[30] The excretion of intact NPs from these pathways is an extremely slow and inefficient process, leading to unwanted accumulation which, in turn, can cause long-term toxicity and interference with common medical diagnoses.[34,35] Exogenous agents inserted in the human body for healthcare treatments have to be completely cleared in a reasonable amount of time, avoiding persistence in the organism.[35] This requisite is currently not fulfilled by any metal based nanoparticle, preventing their translation to the market.[18]

Reducing the size of NPs to ultrasmall range (< 8 nm, ultrasmall nanoparticles, USNPs) is the first principle to enhance their renal clearance efficiency.[19] Many efforts have been done in this direction resulting in a number of interesting findings. This subject is beyond the scope of this review, as other authors have comprehensively reviewed the field.[24,29,36] Despite the interesting excretion kinetics of USNPs, their clearance from the blood-stream is usually excessively fast, reducing their ability to accumulate in targets, and their size is too small to observe the required features for cancer theranostics, hindering a number of applications.[19,29,37] Overall, the dilemma concerning the optimal particle size for clinical applications is still unresolved.[18]

A recent and innovative advance to overcome the issue of unwanted metal accumulation is the ultrasmall-in-nano approach. Within this approach, degradable nanoplatforms comprising USNPs are developed in order to combine the unique properties of noble metal nanoparticles with their excretion by the renal pathway. In this review, the most significant platforms composed by employing the ultrasmall-in-nano approach are reported and discussed. Not surprisingly, all nanoplatforms comprise gold USNPs, mainly due to gold high chemical inertness, broad variety of surface functionalization and straightforward synthesis. It is worth to suggest that an excellent overview on PT application of some degradable nanoplatforms comprising USNPs was recently provided by He et al.[38]

ULTRASMALL-IN-NANO APROACH

In Table 1 is reported a comprehensive overview on the nanoplatforms produced by the ultrasmall-in-nano approach that can be potentially excreted from organisms after the designed action. It is worth to notice that in only three works the amount of metal excreted from murine models have been investigated.[39–41] This demonstrates the groundbreaking nature of ultrasmall-in-nano approach together with the requirement of more investigations in this promising direction.

Polymer-based

Within ultrasmall-in-nano approach, USNPs can be assembled in degradable nano-architectures by employing polymers as assembling agents.[6,38,39,41–57]

One of the first examples in this direction was reported by Tam et al.[42] They described a procedure to assemble gold USNPs (4.1 nm) in aggregates with HD of ~ 83 nm. This was achieved by using a biodegradable triblock copolymer of polylactic acid and polyethylene glycol (PLA(2K)-b-PEG(10K)-b-PLA(2K)) which acted as stabilizer and aggregation agent (Fig. 2-A). These polymer-aggregated USNPs possess a strong NIR extinction, and their biodegradation in cultured cells was investigated by dark-field reflectance and hyperspectral imaging.[42] Furthermore, their feasibility as PA imaging contrast agent was tested in a subsequent work in tissue-mimicking phantoms.[48] These nanoplatforms disassemble in potentially renal clearable USNPs. However, the long synthesis protocol (more than 12h) and the stability concerns related to polymer degradation could represent a severe issue for their widespread employment in clinics. Concurrently, Wang et al. proposed a supramolecular approach to composite size-tunable aggregates of USNPs with enhanced PT efficiency.[53] The system was produced by self-assembly of three building blocks: (i) adamantane (Ad) coated 2 nm gold USNPs, (ii) β-cyclodextrin-grafted polyethylenimine (CD-PEI) and (iii) Ad-functionalized PEG (Ad-PEG). The assemblies

3

showed good stability in the pH range 4-10 and, at physiological pH, in a temperature-range of 7-40 °C. In addition, their size was easily tunable in the range 40-118 nm by varying the ratio of the three building blocks. The aggregates were decorated by a specific targeting peptide able to recognize cells membrane $\alpha_v\beta_3$ receptors. Targeted PTT was evaluated on co-cultured cells containing both $\alpha_v\beta_3$–positive U87 glioblastoma cells and $\alpha_v\beta_3$–negative MCF7 breast cancer cells. Decorated aggregates have demonstrated an enhanced PT efficiency with respect to the control (2 nm Au USNPs) after irradiation with pulsed laser (6 ns, 120 mJ·cm^{-2}). Nevertheless, the optical response of the aggregates is in the range 500-530 nm, far from the first NIR-window, and do not differ significantly from 2 nm Au USNPs. Moreover, the aggregates disassembled at temperatures above 40 °C, raising doubts about their stability and feasibility to perform repeated PT cycles. In the same direction, Yahia-Ammar and co-workers[50] have prepared assemblies (Au-GSH-PAH) of glutathione (GSH) coated gold nanoclusters (GSH-AuNCs) and cationic polymer poly(allylamine hydrochloride) (PAH). The size of the GSH-AuNCs is less than 2 nm, while the size of the aggregates at pH 7 is around 120 nm (Fig. 2-B). The size of the assemblies is pH-responsive, showing reversible shifts from 80 nm at pH 6 to 350 nm at pH 11. These assemblies have demonstrated efficient fluorescence imaging performances triggered by aggregation induced emission (AIE) with a maximum emission around 600 nm. The Authors have also demonstrated the employment of the assemblies as drug delivery vehicles towards TPH1 cells. While these assemblies are not cytotoxic up to 50 μg Au·mL^{-1} for 24h, low cytotoxicity was observed for 250 μg Au·mL^{-1} (below 90% of viability) and 500 μg Au·mL^{-1} (below 80% of viability) for 24h. The pH-dependent resizing of the assemblies could represent an important concern in perspective of clinical use. Indeed, their pharmacokinetics and biodistribution would be significantly altered depending on body localization.[12] Al Zaki and co-workers[41,56] proposed an interesting approach for synthesizing polymeric nanomicelles comprising 1.9 nm gold USNPs (GPMs)

with appealing CT and RT features. Briefly, poly(ethylene glycol) and polycaprolactone amphiphilic diblock copolymers were dissolved in toluene together with gold USNPs, undergoing micellar self-assembly when added to water. The final HD of GPMs is in the broad range 25-150 nm, even though efficient size-sorting in monodisperse sub-populations was achieved through differential centrifugation. 75 nm GPMs were employed as CT contrast and RT radiosensitizer agents both *in vitro* (human fibrosarcoma cells) and *in vivo* (HT1080 flank tumor bearing mice). In particular, a noticeable increase in the amount of DNA double strand breaks ensuing X-ray irradiation was found on cells treated with GPMs. Furthermore, GPMs provided good CT contrast at tumor site, even 48h after intravenous injection, allowing for combined CT/eRT. Notably, RT on mice treated with GPMs afforded a significant increase in median survival, together with a marked decrease of tumor growth. The Authors claim for the possibility of clearance of GPMs after accomplishment of the theranostic action, through biodistribution analyses. They reported that the highest amount of gold was found in the liver one week after the treatment, with a 30-50% of reduction in three months. This result is not surprising, because of the intrinsic hydrophobicity of the USNPs employed, that prevents their complete excretion by the renal pathway. Recently, Cheheltani *et al.*[51] reported the synthesis of a nanomaterial (Au-PCPP) composed by gold USNPs assembled with polymers (Fig. 2-C). The synthesis is performed by using a microfluidic system that provides a good control over the size of Au-PCPP and the loading of gold USNPs. This biocompatible and biodegradable nanoplatform is composed by gold USNPs coated by reduced L-glutathione (GSH, 2.2 nm) or 11-mercaptoundecanoic acid (11-MUA, 5.1 nm), and encapsulated by poly di(carboxylatophenoxy)phosphazene (PCPP). The size of the complete nanoplatform (500-40 nm) is controlled by the amount of methoxy-poly(ethylene glycol)-block-poly(L-lysine hydrochloride) (PEG-PLL) introduced during the reaction.
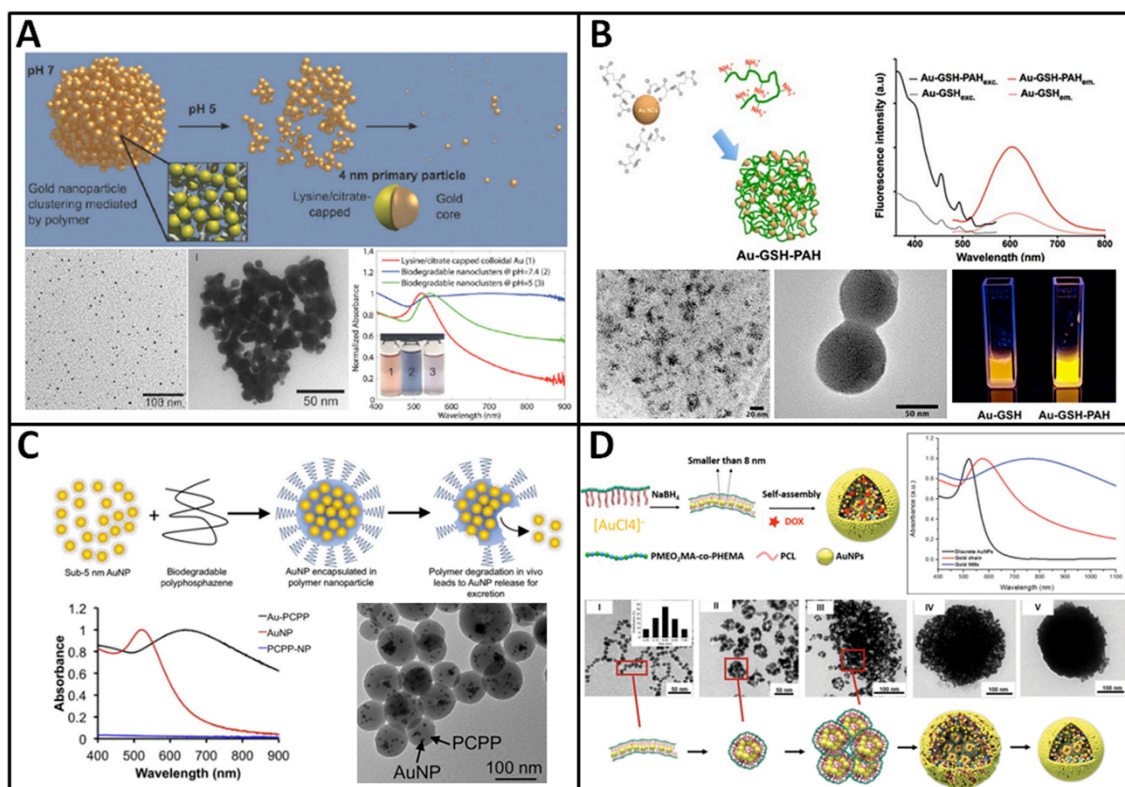
4

Figure 2. Examples of USNPs assembled in nano-architectures by employing polymers. Panel A: top) Scheme for the degradation of pH-responsive aggregates composite by 4 nm gold USNPs and biodegradable polymers. Bottom) TEM images of 4 nm lysine/citrate-capped gold USNPs before (left) and after (center) aggregation by PLA(2K)-PEG(10K)-PLA(2K). Absorbance spectra (right) of 4 nm lysine/citrate-capped gold USNPs (red line), gold USNPs aggregates at pH 7.4 (blue line) and disassembled platforms upon exposure to pH 5 (green line).[42] Panel B: top) scheme of the assembly of glutathione-coated Au USNPs (Au-GSH) by crosslinking with PAH polymer (Au-GSH-PAH) (left) and excitation and emission spectra of Au-GSH (dashed lines) and Au-GSH-PAH (solid lines) (right). Bottom) TEM images of Au-GSH (left), Au-GSH-PAH (center) and sample photo of enhanced fluoresce upon aggregation.[50] Panel C: top) scheme for the production of biodegradable assemblies (Au-PCPP) composed by gold USNPs and poly di(carboxylatophenoxy)phosphazene (PCPP). Bottom) Absorbance spectra (left) of Au-PCPP (black line), AuNP (red line) and PCPP nanoparticles (blue line), and typical TEM image (right) of Au-PCCP.[51] Panel D: top) Schematic representation of the synthesis of DOX@Gold nanomicelles (NMs) (left) and absorbance spectra (right) of 6 nm AuNPs (black line), gold chain composed of AuNPs (red line) and gold NMs (blue line). Bottom) TEM images of the formation of DOX@Gold NMs during 1 h dialysis.[39] Panels A and B were adapted from refs. 37 and 50 with permission of American Chemical Society. Panel C was adapted from ref. 51 with permission from Elsevier. Panel D was adapted from ref. 39 with permission from John Wiley & Sons.

Table 1. Summary of nanoplatforms composed by ultrasmall-in-nano approach with potential theranostic applications.

Nanoplatform[a]	Materials	Size (metal size)[b]	Tested on	Toxicity	Investigated application	Refs.
POLYMERS						
Gold nanoclusters	Citrate capped USNPs aggregated with PLA(2K)-b-PEG(10K)-b-PLA(2K)	83.0[c] (4.1)	Cell line: J477A.1	nr	Dark-field reflectance and hyperspectral imaging, contrast agents in PA imaging	Tam *et al.*[42,48]
AuNR vesicles	AuNRs coated with PEG and PLGA self-assembled by using an oil-in-water method	≈60[c] (8x2)	Cell line: U87MG **Model:** U87MG tumor-bearing nude mice	***In vitro:*** Non-toxic for 24h up to 2 nM of AuNR@PEG/PLGA ***In vivo:*** No obvious inflammation or damage of major organs (heart, liver, spleen, lung, and kidneys) after 10 days treatment	PET (for ^{64}Cu-labeled vesicles) and PA imaging; PT (*in vitro* and *in vivo*)	Song *et al.*[49]
RGD-Au-SNP	Self-assembly of Ad-coated gold USNPs, CD-grafted PEI and Ad-functionalized PEG	40-118 (2)	**Cell lines:** U87 and MCF7	nr	PTT (potential: controlled release, assemble other inorganic NPS)	Wang *et al.*[53]
GPMs[d]	PEG-PCL micelles containing gold USNPs	25-150[c] (1.9)	Cell line: HT1080 **Model:** HT1080 flank tumor-bearing mice	Non-toxic up to 650 mg Au·Kg^{-1} on healthy mice	*In vivo* and *in vitro* CT and RT	Al Zaki *et al.*[41,56]
Au-SPNs	Hydrophobic gold NPs with PLGA assembled with EGG-PG and DSPE-PEG-OCH$_3$	100-180 (6)	**Cell lines:** SUM189 and U87	nr	PTT	Iodice *et al.*[55]
Au-GSH-PAH	Self-assemblies of GSH-AuNCs and PAH	120[c] (< 2)	Cell line: TPH1	***In vitro:*** No cytotoxicity up to 50 µg Au·mL^{-1} for 24 h; low cytotoxicity for 250 and 500 µg Au·mL^{-1} for 24h	Cellular drug delivery and fluorescence imaging in confocal laser scanning microscopy	Yahia-Ammar *et al.*[50]
Au-PCPP	Gold USNPs coated by GSH or 11-MUA encapsulated by PCPP; size controlled by the amount of PEG-PLL	40-500 (2.2 for GSH/5.1 for 11-MUA)	**Cell lines:** HEPG2, Renca and SVEC4-10EHR1 **Model:** C57BL/6J mice	***In vitro:*** No cytotoxicity up to 1.0 mg Au·mL^{-1} for 8h	*In vitro* and *in vivo* CT and PA dual imaging	Cheheltani *et al.*[51]
DOX-EGF-SA-AuNPs	Gold USNPs coated by TOAB self-assembled with a mix of HS-PEG-SH and mPEG-SH	86.8 (6.5)	**Cell lines:** U87, GBM43 and U251 **Model:** Male nude mice with U87 brain tumor model	***In vitro:*** No inhibitive effects on U87 cells at 25 nM Au for 72h (without DOX)	*In vitro* and *in vivo* pH-responsive drug release	Feng *et al.*[52]
Au@PLA-(PAH/GO)$_n$	Gold USNPs assembled with PLA in camphor microcapsules embedded in layer-by-layer absorbed PAH and GO	1500 (2.6/2.8)	**Cell line:** HeLa (PT investigations) and HUVECs (cytotoxicity) **Model:** New Zealand white rabbit and mice bearing HT1080 tumor	***In vitro:*** No evident from 0.01 to 1 mg·mL^{-1}	***In vitro:*** Contrast agent to simultaneously enhance real-time US imaging and phantom CT ***In vivo*** (rabbit): US imaging ***In vivo*** (mice): CT and PTT	Jin *et al.*[54]

6

	Name	Description	Size[a,b]	Cell lines / Model	In vitro toxicity	Application	Ref.
	DOX@Gold NMs[d]	Assemblies of DOX@gold NMs and comb-like amphipathic polymer composed of biodegradable hydrophobic PCL/PHEMA and hydrophilic PMEO$_2$MA	300 (6.1)	**Cell lines:** MCF7, L929 and HUVEC **Model:** Mice bearing MCF7 tumors	*In vitro:* More than 80% of cell viability (for all the 3 cell lines) up to 2 mg·mL^{-1} for 24h (gold NMs without DOX)	*In vivo:* combined chemotherapy and PT therapy; PA and CT	Deng *et al.*[39]
	PLGA-AuNCs	PLGA NPs containing AuNCs capped with 11-MUA and MUD; this NPs were coated with a mixture of PEG: soybean lecithin.	66-117[c] (8)	**Cell line:** J774A.1	nr	*In vivo* CT contrast agent	Mieszawska *et al.*[57]
SILICA	QRs	Hollow MSN containing AuNPs in the cavity and gold USNPs in the channels	150 (< 2 for Au USNPs, 7.3 average crystallite size for AuNPs)	Cell lines: HeLa **Model:** CD1 nu/nu mice bearing LS174T-luc tumor model	*In vitro:* No significant up to 40 µg·mL^{-1} after 3 days	*In vitro:* NIR fluorescence imaging, drug delivery and PDT *In vivo:* NIR fluorescence, 3D-PA and MRI; drug delivery and PDT	Hembury *et al.*[58]
	GEM/DOX or HOE loaded MSN-AuNC@BSA	MSN and BSA-coated Au USNPs as nanogates for MSN pores	257[c] (3.7)[c]	**Cell lines:** HeLa, A549, PANC-1 **Model:** Nude mice bearing MIA Paca-2 subcutaneous tumor	*In vitro:* Biocompatible up to 100 µg·mL^{-1}	*In vitro:* Nuclear staining *In vivo:* Fluorescence imaging and dual drug delivery of GEM and DOX	Croissant *et al.*[59]
	Passion fruit-like Nano-Architectures	Biodegradable silica nanocapsules comprising PSS-coated USNPs aggregated by PLL	97.6 (2.8)	Cell line: MIA PaCa-2	*In vitro:* Biocompatible up to 50 µg·mL^{-1} for 24h; more than 80% of cell viability up to 10 µg·mL^{-1} for 48h and 72h	Drug delivery and PA (potential: PET, CT, eRT, US)	Cassano *et al.*[60,61]
OTHERS	LiposAu NPs[d]	DSPC:CHOL liposomes comprising gold USNPs as shell	100[c] (< 5)	**Cell lines:** MDA-MB-231, L929, NIT-3T3, MCF7-*fluc2-turboFP* and HT1080-*fluc2-turboFP* **Model:** Swiss albino mice (biodistribution), BALB/c NUDE mice (PT efficacy using HT1080-*fluc2-turboFP* tumor xenograft)	*In vitro:* non-toxic in L929 and NIT-3T3 cells even at 1 mg·mL^{-1} of Lipos Au (lipid concentration)	*In vitro:* Drug delivery, optical imaging (with NIR dye), PT, and CT *In vivo:* PT therapy	Rengan *et al.*[40,62]
	AuNPs/LDHs	LDHs containing gold USNPs	150 (≈3.5)	**Cell line:** Hepatoma-derived HepG2.2.2.15 cells for viral replication	Non-toxic up to 125 µg·mL^{-1}	Antiviral action against HVB	Carja *et al.*[63]
	LGAuNPs LGAuNPs-Co	BSA/GSH-coated gold USNPs assembled with Co^{2+}ions	12.2-7.5 (3.6)[c]	**Cell lines:** HepG2, LO2, A549, and 4T1 cell lines **Model:** female Balb/c mice	Non-toxic up to 10.0 mg·mL^{-1} in 6–24 h range	*In vivo* and *in vitro* fluorescence imaging	Lai *et al.*[64]

[a]As described in the reference; [b]expressed in nm; [c]hydrodinamic diameter; [d]excretion test; not reported (nr); X-ray computed tomography (CT); photodynamic therapy (PDT); magnetic resonance imaging (MRI); photoacoustic (PA); ultrasound (US); positron emission tomography (PET); enhanced radiation therapy (eRT); mesoporous silica nanoparticles (MSN); gold nanoclusters (AuNCs); gold nanorods (AuNRs); gold nanoparticles (AuNPs); graphene oxide (GO); layered double hydroxides (LDHs); hepatitis B virus (HVB); bovine serum albumin (BSA); doxorubicin (DOX); nanomicelles (NMs); gemcitabine (GEM); reduced L-glutathione (GSH); 11-mercaptoundecanoic acid (11-MUA); 11-mercapto-1-undecanol (MUD); tetraoctylammonium

7

bromide (TOAB); triblock copolymer of polylactic acid and polyethylene glycol (PLA(2K)-b-PEG(10K)-b-PLA(2K)); poly(ethylene glycol) (PEG); poly (lactic acid-co-glycolic acid) (PLGA); L-α-phosphatidyl-DL-glycerol (EGG-PG); 1,2-distearoyl-sn-glycero-3-phosphoethanolamine-N-[carboxy(polyethylene glycol)-2000] (DSPE-PEG-OCH$_3$); adamantane (Ad); β-cyclodextrin (CD); polyethyleneimine (PEI); poly(lactic-co-glycolic acid) (PLGA); poly(allylamine hydrochloride) (PAH); poly di(carboxylatophenoxy)phosphazene (PCPP); methoxy-poly(ethylene glycol)-block-poly(L-lysine hydrochloride) (PEG-PLL); dithiol-polyethylene glycol (HS-PEG-SH); methoxy polyethylene glycol thiol (mPEG-SH); poly(ε-caprolactone) (PCL); poly(2-hydroxyethyl methacrylate) (PHEMA); poly[2-(2-methoxyethoxy) ethyl methacrylate] (PMEO$_2$MA); poly-lactic acid (PLA); poly(sodium 4-styrenesulfonate) (PSS); poly(L-lysine) (PLL); 1,2-distearoyl-sn-glycero-3-phosphocholine:cholesterol (DSPC:CHOL).

1
2
3
4
5
6
7
8
9
10
11
12
13
14
15
16
17
18
19
20
21
22
23
24
25
26
27
28
29
30
31
32
33
34
35
36
37
38
39
40
41
42
43
44
45
46

8

The optical response of the assemblies is tunable in the range 600-900 nm by modifying the gold USNPs loading. These nanoplatforms were successfully employed as *in vitro* (HEPG2, Renca and SVEC4-10EHR1 cell lines) and *in vivo* (C57BL/6J mice) CT and PA dual imaging contrast agents. However, the CT attenuation rate (52.3 HU·mg^{-1}) does not lead to a significant improvement compared to gold nanoparticles loaded lipoproteins reported in previous works from the same group.[65] Despite the interesting control over the behavior of the final product, no investigations on biodistribution and excretion were reported. A similar strategy was explored also by Deng and co-workers (Fig. 2-D).[39] They have produced gold USNPs (6.1 nm) assembled in doxorubicin (DOX) loaded nanomicelles (300 nm, DOX@Gold NMs) by using a comb-like amphipathic polymer composed of biodegradable hydrophobic poly(ε-caprolactone) (PCL)/poly(2-hydroxyethyl methacrylate) (PHEMA) and hydrophilic poly[2-(2-methoxyethoxy) ethyl methacrylate] (PMEO$_2$MA). The DOX@Gold NMs assembly was strictly dependent to the post-processing procedures. The Authors have demonstrated that Gold NMs (without

DOX) show low-toxicity on three different cell lines (MCF-7, L929 and HUVEC) up to a concentration of 2 mg·mL^{-1}. Indeed, cell viability was more than 80% after incubation for 24h. DOX@Gold NMs have the LSPR in the NIR region (600-1100 nm). This nanoplatform was suggested for both diagnostics and therapy of neoplasms. It was successfully employed in murine models as multimodal contrast agents for PA imaging and CT. DOX@Gold NMs were also tested as drug carriers *in vitro* (MCF-7 cells) and for combined PTT and chemo-therapy in murine models bearing MCF-7 tumors. The Authors claim for the potential renal clearance of their nanoplatform, but no evidences are reported. The major concern is related to the potential protein corona formation on gold USNPs after the degradation of the nanoplatform, that can greatly increase the HD, hampering the possibility of excretion. Moreover, metal melting and re-shaping is commonly observed after laser irradiation on the LSPR, resulting in the formation of metal nanoparticles with increased size and different shape.[61,66] This phenomenon can significantly reduce the potential excretion of DOX@Gold NMs building blocks.
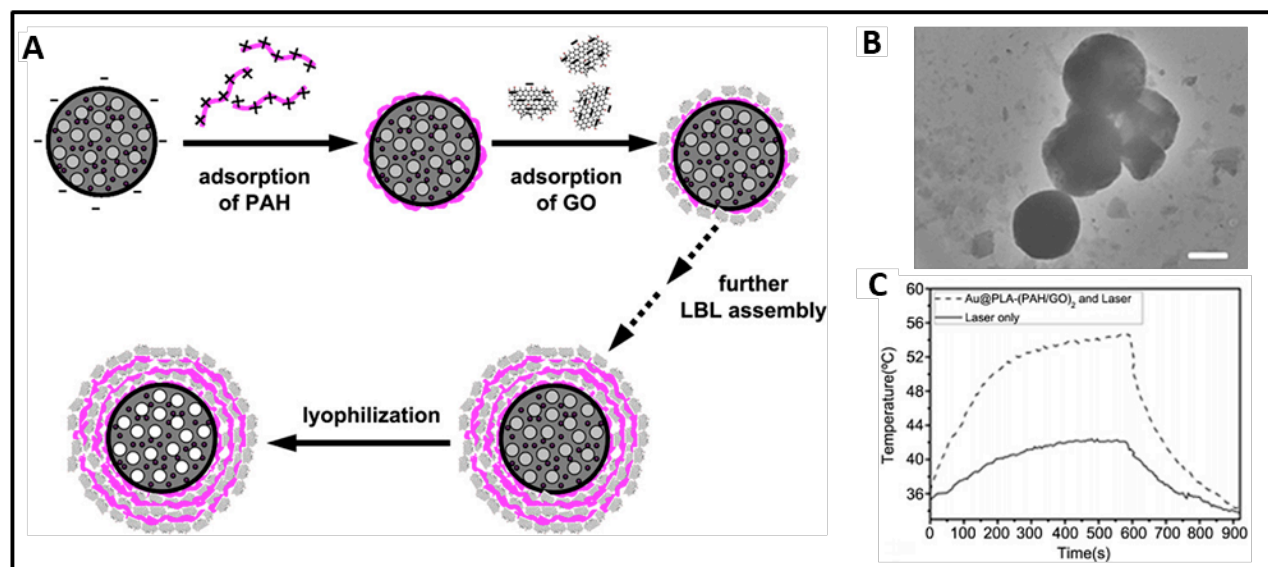

Figure 3. A) Synthesis of Au@PLA-(PAH/GO)$_n$ microcapsules by layer-by layer (LbL) technique. B) TEM image of Au@PLA-(PAH/GO)$_2$. C) Temperature curves during photothermal treatment (808 nm laser, 2.23 W·cm^{-2}) of mice bearing HT1080 tumor with intratumoral injection of saline solution or Au@PLA-(PAH/GO)$_2$ microcapsules.[54] Adapted from ref. 54 with permission from Elsevier.

Another interesting example was developed by Jin *et al.*[54] The Authors (Fig. 3) have prepared microcapsules containing gold USNPs, in which graphene oxide (GO) and poly(allylamine hydrochloride) (PAH) were adsorbed via layer-by-layer (LbL) technique (Au@PLA-(PAH/GO)$_n$, where n=number of PAH/GO layers). These assemblies have demonstrated no significant cytotoxicity against HUVECs cells in the range of 0.01 to 1 mg·mL^{-1}. Moreover, promising *in vitro* and *in vivo* results are reported for their employment as real-time US and

CT contrast agents and for PT treatment of mice bearing HT1080 tumor. However, the Authors have not reported biodistribution nor excretion investigations. Moreover, the size of the nanoplatform is in the micron range, reducing the possible theranostics applications. An interesting approach using anisotropic NPs was adopted in 2015 by Song and co-workers, who described the preparation of biocompatible and biodegradable nanoplatform (Fig. 4A) composed by gold nanorods (AuNRs, ~8x2 nm) coated by poly(ethylene glycol)

(PEG) and poly(lactic-co-glycolic acid) (PLGA) (~60 nm).[49] AuNRs assemblies have the LSPRs in the NIR region (Fig. 4B), and their employment as PA and PET contrast agent (the latter after labeling by ^{64}Cu) and PT agent demonstrated in U87MG tumor-bearing nude mice (Fig. 4C).
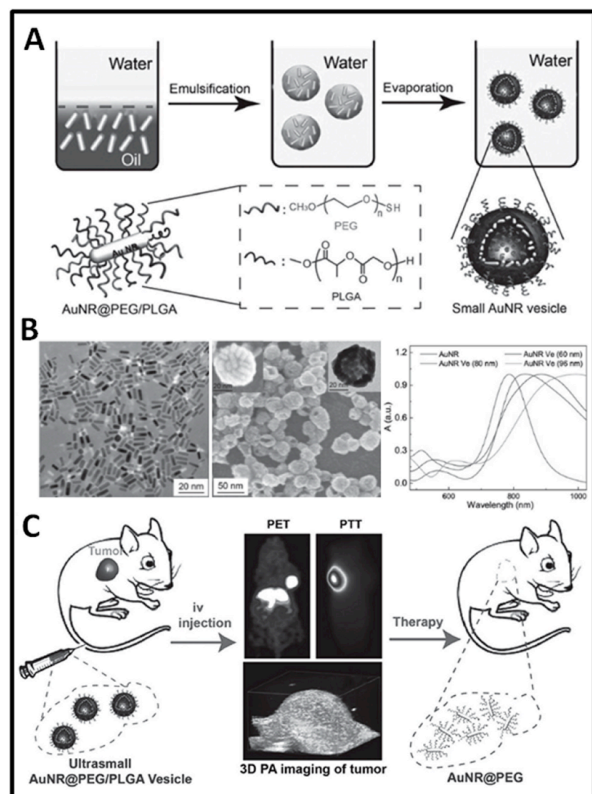

Figure 4. A) Scheme for the preparation of AuNR@PEG/PLGA and the formation of the self-assembled vesicles using oil-in-water method. B) TEM images of AuNR@PEG/PLGA (left) and the self-assembled vesicles (center) and relative absorbance spectra (right). C) Cartoon relative to *in vivo* employment of self-assembled vesicles for PET, 3D PA imaging, and PTT of tumor bearing mouse.[49] Adapted from ref. 49 with permission from John Wiley & Sons, Inc.

The Authors have also reported a high passive accumulation in tumor after intravenous administration, due to the nanoplatform size and charge. It is worth to notice that a considerable amount of AuNRs (more than 10% ID·g^{-1}) was found in reticulo-endothelial system (RES) after 10 days from the intravenous injection, together with not negligible amount of gold in lungs, kidneys and blood (2.5% ID·g^{-1} each). It would be interesting to perform more investigations in order to better shed light on the pharmacokinetics and excretion of this kind of nanoplatforms. It is useful to notice that living cell investigations with these nanoplatforms have revealed that also AuNRs suffers from re-shaping during 6 minutes irradiation at 808 nm (power: 0.8 W·cm^{-2}). Also in this case, irradiation on the LSPR can induce growing of USNPs, preventing excretion of metals from organisms.

Silica-based

The main hurdles with polymer-based nanoplatforms are related to stability concerns and surface decoration with moieties of interest. An appealing approach to overcome these issues is the formation of a silica shell around the metal aggregates. Indeed, silica can be employed both as shielding agent and as straightforward modifiable surface. Moreover, silica is biodegradable and non-toxic.[67,68] Silica has been generally recognized as safe by the FDA, it is currently used as a food additive in various products, and it is part of the diet of people through vegetables.[67] Some types of silica nanomaterials, *e.g.* those produced *via* sol-gel methods, are hydrolytically unstable and dissolve over time into water-soluble silicic acid (Si(OH)$_4$, pKa 9.6).[67] Silicic acid is then excreted in the urine or used from organisms to maintain bone health.[67]
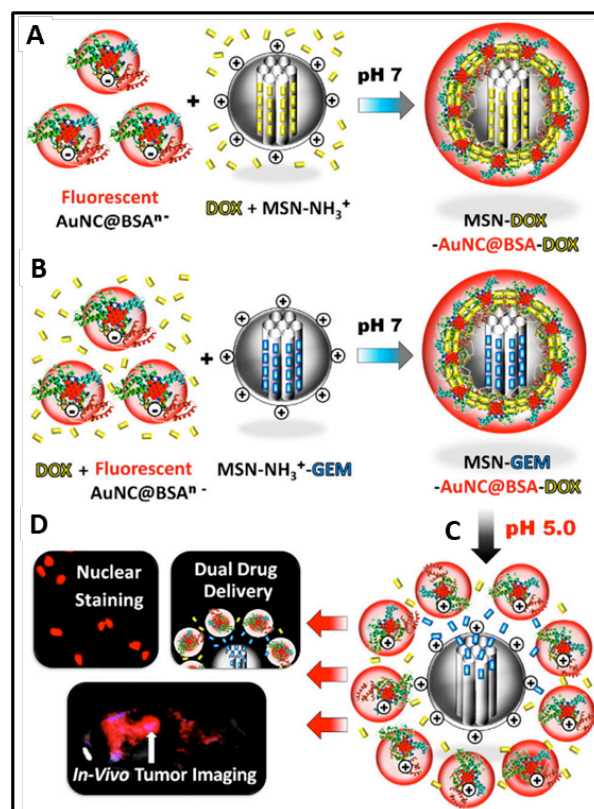

Figure 5. Scheme of the production of A) DOX-loaded MSN-AuNC@BSA, and B) GEM-DOX-loaded MSN-AuNC@BSA. C) Disassembly of GEM-DOX-loaded MSN-AuNC@BSA triggered by acidic environment. D) Possible applications of dual drug-loaded MSN-AuNC@BSA.[59] Reprinted from ref. 59 with permission from Elsevier.

Silica nanocapsules offer a surface that is modifiable/functionalizable by standard and fast techniques with moieties of interest, such as targeting

agents, increasing their possible accumulation in cancer targets.[60,67] One of the first examples in this direction are the quantum rattles (QRs). These versatile nanosystems were recently developed by Hembury *et al.*[58] They have produced hollow mesoporous silica spheres (d≈150 nm) with shell thickness of ~25 nm comprising a mixture of fluorescent gold quantum dots (AuQDs, < 2nm) and gold NPs bigger than 8 nm embedded in the mesoporous silica. This nanoplatform was biocompatible (no significant cell deaths up to 40 $\mu g \cdot mL^{-1}$ after 3 days) and has demonstrated an enhanced drug encapsulation capability. For example, doxorubicin (DOX) encapsulation was nearly twice (15.1% wt/wt) with respect to optimized liposomal-DOX systems (7.8%). Furthermore, AuQDs are paramagnetic and emit light in the NIR region resulting in promising agents for multimodal real-time imaging (NIR fluorescence, PA and MRI). The Authors have demonstrated these features both in HeLa cells and in CD1 nu/nu mice bearing LS174T-luc tumor model. This system has also provided an interesting platform for PTT. Despite the appealing behaviors of this nanoplatform, the presence of AuNPs bigger than 10 nm strongly reduced their potential applications, due to accumulation and excretion concerns. Another recent example involving

silica and USNPs was provided by Croissant and co-workers.[59] In this approach, mesoporous silica nanoparticles (MSN) were loaded with gemcitabine (GEM) and/or DOX, and then coated with gold nanoclusters in BSA (AuNC@BSA). AuNC@BSA were employed as pH-sensitive nanogates (pH 7 closed, pH 5 opened) for drug controlled release (Fig. 5). This nanoplatform has demonstrated a massive dual drug loading (72% wt/wt), higher than the ones reported for liposomes and polymers, respectively 10% and 12% wt/wt.[69,70] Moreover, the system was stable in blood serum, since it was observed less than 3% of drug leakage after one week. It would be noticeable to perform these investigations *in vivo*, to better understand the drug leakage in a complex matrix. Drugs are loaded both inside MSN and in the AuNC@BSA layer. Hence, the spatial segregation of drugs in two different compartments allows this system to well-suite for controlled dual-cargo release. The system has demonstrated good biocompatibility in A549, PANC-1 and HeLa cells (up to 100 $\mu g \cdot mL^{-1}$) after 24h incubation. The tumor accumulation after intravenous injection was significant, but no biodistribution at longer times neither biodegradation of MSN was shown, lacking a better understanding of the pharmacokinetic behavior for these nanomaterials.
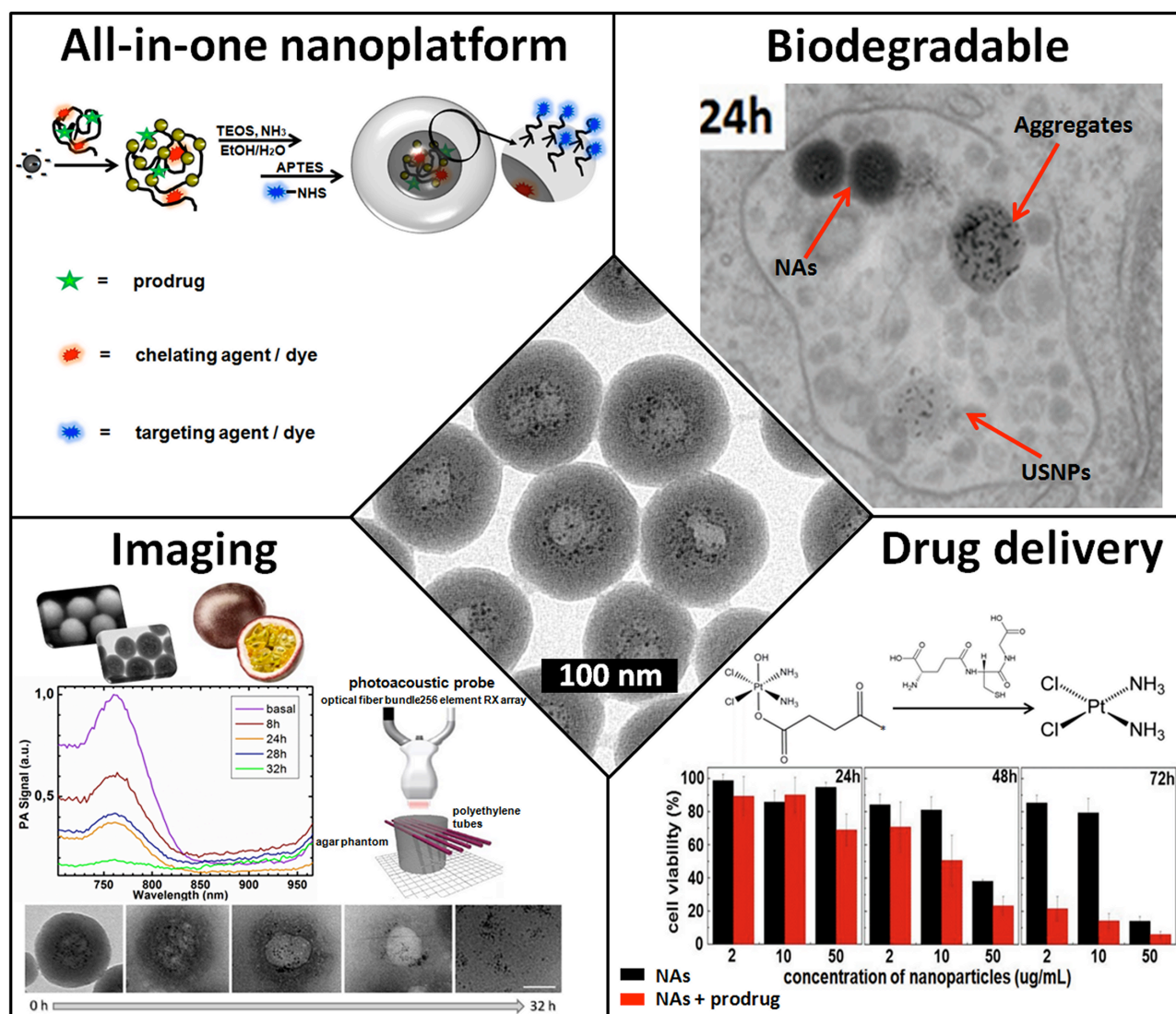
11

Figure 6. Typical TEM image of passion fruit like nano-architectures (NAs) (center) and their main features. Clockwise from top-left: scheme of the production for all-in-one nanoplatforms, biodegradation of NAs in cellular environment, PA imaging during degradation in phantoms, and *in vitro* drug delivery of endogenous GSH-triggered cisplatin prodrug.[60,61] Adapted from refs. 60 and 61.

A recent intriguing example of silica degradable nanomaterials is the nature-inspired passion fruit-like nano-architectures (NAs). NAs strengths are: i) versatility, ii) low cost, iii) possible scale-up, and iv) easy synthesis protocol (just 3.5h) and storage (Fig. 6).[60,61,68,71,72] NAs are composed of 100 nm hollow silica nanospheres embedding plasmonic USNPs in a polymeric functional matrix, resembling this exotic fruit.[68,71] In NAs, the silica shell gives to the system the best size to enhance their accumulation in tumor targets, and provides a straightforward modifiable/functionalizable surface.[60] Strictly packed USNPs confer the physical behavior needed for theranostic applications,[61] while the polymer can be covalently functionalized with active molecules without affecting its rolling properties.[60] NAs biodegrade in both physiological fluids and cellular environment in less than 48h to low-toxic and renal clearable building blocks: biodegradable polymers, endogenous-GSH coated USNPs and silicic acid.[60,67,73] Moreover, NAs offer a multifunctional platform for both therapy and diagnostic of neoplasms.[60,61] For example, NAs are designed to contain 5-18% w/w of metals (among which gold, platinum, silver or their mix).[71,72] Thus, NAs could be employed as agents for CT-guided RT treatment, enhancing the RT efficacy and minimizing the energy deposition in surrounding healthy tissues.[74–76] Furthermore, NAs can comprise molecules required for chemotherapy or PA imaging or PET, such as, respectively, drugs, dyes and chelating agents. The inclusion in NAs of cisplatin in its oxidized form as an endogenously-triggered prodrug has demonstrated an increased efficacy on Mia PACA-2 cell-line.[60] Accordingly, NAs may be employed for both localized chemo(radio)-therapy and multiple imaging diagnosis (CT and PET) to

12

allow in-depth analysis of clinically relevant biological phenomena before or during the therapeutic action. So far, NAs have been employed *ex vivo* as PA contrast agents, establishing a novel paradigm for the composition of exogenous PA probes based on the interaction between commercial IR-dyes and USNPs.[61,77] Overall, NAs result as one of the most appealing candidate for the translation of metal nano-theranostics to clinics.

Others

Another promising strategy to develop excretable nanoplatform by the ultrasmall-in-nano approach is by employing liposomes.[8,38,40,62,78–81] A liposome is a spherical vesicle having at least one lipid bilayer. The liposomes can be used as vehicles for administration of nutrients and drugs.[78] Recently, Rengan *et al.*[40,62] reported a protocol (Fig. 7) to obtain biodegradable and biocompatible 1,2-distearoyl-*sn*-glycero-3-phosphocholine: cholesterol (DSPC:CHOL) liposomes coated with USNPs (LiposAu NPs). The nanoplatform also comprises indocyanine green (ICG, an FDA approved NIR dye) and showed an extinction band in the NIR due to the LSPR coupling of gold USNPs, providing appealing optical features to the assembly. *In vitro* tests on L929 and NIT-3T3 cells reported no toxicity even at a concentration of 1 mg·ml^{-1} for 48h incubation. LiposAu NPs performance in PT treatment were investigated both *in vitro* on living MCF-7 (breast) and HT1080 (fibrosarcoma) cells and *in vivo* on BALB/c NUDE mice HT1080-*fluc2-turboFP* tumor xenograft model. Moreover, LiposAu NPs were successfully employed as drug carriers and CT contrast agents in cultured cells and phantoms, respectively. LiposAu NPs biodistribution and clearance were investigated in health Swiss albino mice. In agreement to their size (∼200 nm), the very first accumulation after the injection of these assemblies was in the RES. After 14 days, the amount

of gold found in mice liver and kidneys was, respectively, 3% and 0.22% ID. Likely, USNPs released by LiposAu NPs underwent protein corona formation, increasing the HD and modifying the superficial charge. This phenomenon may contribute to the failure in the complete metal excretion during that timeframe. Assemblies of USNPs were also achieved by employing layered double hydroxides (LDHs)[63] or cations.[64] LDHs comprising various metals (Mg, Zn, MgFe) and gold USNPs were successfully produced and investigated for the treatment of hepatitis B virus (HBV).[63] This work fits with the subject of this review because HBV is strongly correlated to liver cancer. The Authors have developed a synthetic protocol to directly achieve gold USNPs (≈3.5 nm) on the surface of LDH particles (≈150 nm, AuNPs/LDHs). The antiviral effect of this nanoplatform was successfully investigated against HBV and hepatoma-derived HepG2.2.215 cells. AuNPs/LDHs are able to reduce the amount of viral and subviral particles up to 80%. The highest efficacy (around 90%) was achieved by AuNPs/LDHs comprising manganese and iron cations. Moreover, the nanoplatforms are non-toxic for concentrations up to 125 μg·mL^{-1}. However, also in this case, biodistribution and excretion investigations are not provided.

GENERAL CONSIDERATIONS

In this section, some general considerations on clinical translation of nanomaterials are provided. The key-question for FDA, EMA or PDMA/MHLW approbation of a novel nanomaterial is whether all its components are completely cleared and in which time frame.[82] Leaving residues in patients is not acceptable, unless the novel material is reported as a device.[82] In this review, we have comprehensively discussed this key-question and the approach to
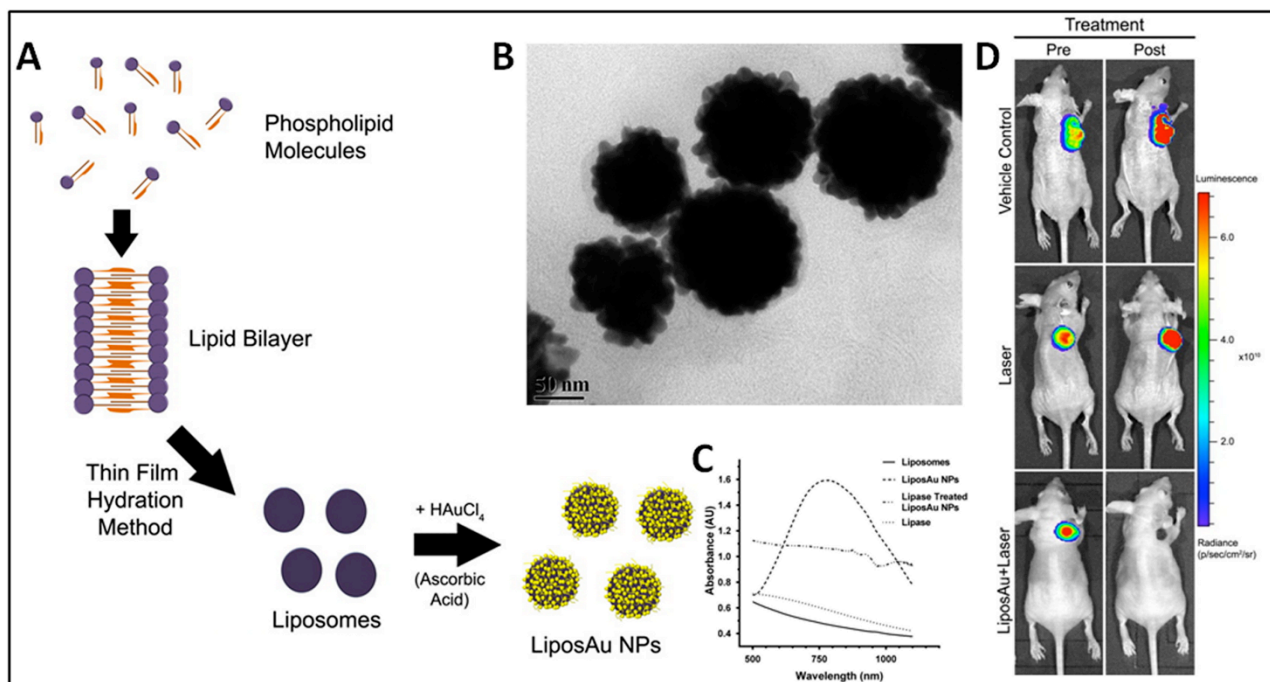
13

Figure 7. A) Scheme of the production and B) TEM image of gold USNPs-coated liposomes (LiposAu NPs); C) Absorbance spectra of lipase, liposome, and LiposAu NPs treated with lipase enzyme in comparison with LiposAu NPs (untreated). D) *In vivo* bioluminescence images before and after PT treatment of mice bearing HT1080-*fluc2-turboFP* tumor xenografts.[40] Adapted from ref. 40 with permission of American Chemical Society.

unlock the features of metal nanomaterials for healthcare. On the other hand, other concepts should be considered. Besides size, also shape, surface properties and mechanical stiffness ("4S parameters") of nanomaterials are critical parameters for vascular residence, tumor accumulation and phagocytic sequestration.[30,83]

In the last years, lacks of sufficient knowledge of the regulatory and industrial requirements for development of healthcare products has led to the failure of most of the proposed nanoplatforms.[82] The usual pipeline of a nanomaterial - from the idea to the market - passes through its on-bench development, pre-clinical and manufacturing validation, and to clinical pilot and phase II/III validation. Only the most promising materials go into costly pre-clinical and following assessments. On this hand, the story of Doxil development is very inspirational for the design of next generation nano-theranostics.[84]

To attract industrial interests a nanomaterial must work and work safely. It has to meet good manufacturing practice (GMP) standards, be ready to be scalable (it is likely that the eventual GMP batch will be up to 1 kg in the pre-clinical phase), works better compared to the standard of care, adhere to regulatory analytical requirements, be stable and reproducible (with all impurities, surfactants, and other involved molecules known and quantified), be simple (the more complex the material, the higher the risks of pre-clinical failure), and be flexible and transferable.[82,85] Furthermore, a complete set of

absorption/distribution/metabolism/excretion (ADME) investigations has to be fully provided in both a rodent species and larger animal models.[83,86] Although a significant number of nanomaterials for healthcare has been approved in the last decades, there is still a lack of specific general protocols for their preclinical assessment.[87–89] Global regulatory trends are yet to be defined, and, as alternative, the first approaches employed on preclinical safety/toxicology for small molecules have been frequently adapted to evaluate the behaviors of nanomaterials.[90,91] However, to date it is generally acknowledged that the standard development program applied to demonstrate therapeutic equivalence for small, well-characterized molecules, cannot be straightly applied to complex drugs.[91]

Indeed, nanomaterials are complex 3D-constructs comprising multiple components with preferred spatial arrangements.[82,92] Owing to the complexity of nanomaterials compared to small homo-molecular substances, the existing regulatory framework allows specific considerations of each new candidate on a product-by-product basis.[87,93] This is consistent with the recently published protocol of regulatory agencies.[93] Such an evaluation strategy is necessary due to the diversity in characterization, physicochemical properties, and biological interactions of different types of nanomaterials involved.[93] Furthermore, profound knowledge and characterization of these complex products is needed in order to avoid unpredicted effects on patients, such

14

as potential immune reactivity.[90] It is worth to remember here that in the nano-range, small size/shape-changes result in giant behavioral changes.[87] On this hand, standardized and robust quality control protocols and assays have to be produced and validated in order to effectively monitor and characterize not only the physicochemical features of nanomaterials, among which size, dispersion, morphology and charge, but also to assess their performance, metabolism assessment, pharmacokinetics, specific cellular uptake, interaction with immune cells and organisms.[87,88,90] Furthermore, interactions between experimental and computational scientists could greatly enhance the predictive accuracy of the investigations and speed-up the development process. Complete discussions on the parameters for quality and safety evaluation of nanotechnology-based medicinal products for biomedical use, together with many reasoning cues, are provided in some recent works.[82,83,88,90]

Overall, in order to produce standard guidelines, international cooperation and harmonized strategies between regulatory agencies are desirable to boost this promising and fast-growing field.

PERSPECTIVES

Accumulation in organism after the medical action still remains the major concern for the clinical translation of metal nanoparticles. Renal clearance has been demonstrated to be the most practical pathway to avoid undesirable toxic effects. Ultrasmall-in-nano is a groundbreaking approach for the design of all-in-one nanoplatforms. These novel disassembling nanomaterials would be the key-technology to overcome the concern of safe medical-employment of noble metal nanoparticles while maintaining most of their desirable theranostic moieties. Personalized and effective treatments of neoplasms driven by noble metal nanoparticles may be no longer a dream, but a real possibility in the very next future. Even though the nanoplatforms so far carry on an enormous potential, they are still far from optimization. In particular, the best equilibrium between the optimum efficacy and the desired excretion is generally not reached.

Moreover, it is significant that within the few manuscripts present in literature, only three have reported quantitative investigations on metal excretion. On one hand, this is related to the youngness of the approach. On the other, to the fact that the general main aim of Researchers is often to focus only on the theranostics efficacy, ignoring the fate of metal NPs. In order to boost the generation of efficient low-invasive treatments of neoplasms, a change in the attitude is desirable. Shifting the focus to "what happens after the action" and collaborating closely with clinicians and core-discipline experts

shall be fundamental for the optimum design of translatable metal nanomaterials.

Other important questions remain off-target degradation, protein corona formation, tumor retention, penetration, and cellular internalization. Also, possible scaling-up of nanomaterials, good laboratory practice (GLP) certification, and not last, the cost effectiveness of the scalable approach, should be thoroughly addressed. About the latter, a usual misconception is about the possible final price of noble-metal based treatments. However, the cost of noble metals usually has a little impact on the cost of the final nanomaterial.[26] For example, gold affects the final price of 5% w/w gold-loaded passion fruit-like nano-architectures for 0.2 eurocent/mg of NAs.

These multidisciplinary challenges open up new exciting opportunities and possible networking between Researchers. Furthermore, despite the high "publication pressure" to which Researchers are subjected, ethic and integrity are strictly mandatory. Too often there are retracted manuscripts or manuscripts reporting too little information for the reproduction and extension of data. In particular for the nanomedicine field, Researchers should perform their research by considering they are working on the humanity hopes.

Overall, metal nanomaterials are an extremely promising platform for novel treatments of neoplasms. By employing the ultrasmall-in-nano approach, metal nanomaterials have a real potential to open new horizons in medicine, and to pave the way for new paradigms in the next generation of theranostics.

Conclusion

In this review, the literature on ultrasmall-in-nano approach for the development of clearable metal theranostics is analyzed and discussed. Remarkably, the works on this subject are few and recent, demonstrating its groundbreaking nature. The field is novel, and the resulting gains have the potential to widely revolutionize cancer treatments in the next future.

AUTHOR INFORMATION

Corresponding author

*Email: valerio.voliani@iit.it

Author Contributions

The manuscript was written through contributions of all authors. All authors have given approval to the final version of the manuscript.

Notes

The authors declare no competing financial interest.

15

REFERENCES

(1) Duncan, R., Gaspar, R. (2011) Nanomedicine(s) under the microscope. *Mol. Pharm. 8*, 2101–2141.

(2) Schütz, C. a, Juillerat-Jeanneret, L., Mueller, H., Lynch, I., Riediker, M. (2013) Therapeutic nanoparticles in clinics and under clinical evaluation. *Nanomedicine 8*, 449–467.

(3) Heidel, J. D., Davis, M. E. (2011) Clinical developments in nanotechnology for cancer therapy. *Pharm. Res. 28*, 187–199.

(4) Bobo, D., Robinson, K. J., Islam, J., Thurecht, K. J., Corrie, S. R. (2016) Nanoparticle-Based Medicines: A Review of FDA-Approved Materials and Clinical Trials to Date. *Pharm. Res. 33*, 2373–2387.

(5) Cheng, Z., Al Zaki, A., Hui, J. Z., Muzykantov, V. R., Tsourkas, A. (2012) Multifunctional Nanoparticles: Cost Versus Benefit of Adding Targeting and Imaging Capabilities. *Science (80-.). 338*, 903–910.

(6) Lim, E., Kim, T., Paik, S., Haam, S., Huh, Y., Lee, K. (2015) Nanomaterials for Theranostics: Recent Advances and Future Challenges. *Chem. Rev. 115*, 327–394.

(7) Muhanna, N., Macdonald, T. D., Chan, H., Jin, C. S., Burgess, L., Cui, L., Chen, J., Irish, J. C., Zheng, G. (2015) Multimodal Nanoparticle for Primary Tumor Delineation and Lymphatic Metastasis Mapping in a Head-and-Neck Cancer Rabbit Model. *Adv. Healthc. Mater. 4*, 2164–2169.

(8) Huynh, E., Rajora, M. A., Zheng, G. (2016) Multimodal micro, nano, and size conversion ultrasound agents for imaging and therapy. *Wiley Interdiscip. Rev. Nanomedicine Nanobiotechnology 8*, 796–813.

(9) Lovell, J. F., Jin, C. S., Huynh, E., Jin, H., Kim, C., Rubinstein, J. L., Chan, W. C. W., Cao, W., Wang, L. V., Zheng, G. (2011) Porphysome nanovesicles generated by porphyrin bilayers for use as multimodal biophotonic contrast agents. *Nat. Mater. 10*, 324–332.

(10) Ng, K. K., Takada, M., Jin, C. C. S., Zheng, G. (2015) Self-Sensing Porphysomes for Fluorescence-Guided Photothermal Therapy. *Bioconjug. Chem. 26*, 345–351.

(11) Huynh, E., Jin, C. S., Wilson, B. C., Zheng, G. (2014) Aggregate enhanced trimodal porphyrin shell microbubbles for ultrasound, photoacoustic, and fluorescence imaging. *Bioconjug. Chem. 25*, 796–801.

(12) Longmire, M., Choyke, P. L., Kobayashi, H. (2008) Clearance properties of nano-sized particles and molecules as imaging agents: considerations and caveats. *Nanomedicine 3*, 703–717.

(13) Black, K. C. L., Wang, Y., Luehmann, H. P., Cai, X., Xing, W., Pang, B., Zhao, Y., Cutler, C. S., Wang, L. V, Liu, Y., Xia, Y. (2014) Radioactive 198Au-Doped Nanostructures with Different Shapes for In Vivo Analyses of Their Biodistribution, Tumor Uptake, and Intratumoral Distribution. *ACS Nano 8*, 4385–4394.

(14) Xiao, K., Li, Y., Luo, J., Lee, J. S., Xiao, W., Gonik, A. M., Agarwal, R. G., Lam, K. S. (2011) The effect of surface charge on in vivo biodistribution of PEG-oligocholic acid based micellar nanoparticles. *Biomaterials 32*, 3435–3446.

(15) Blanco, E., Shen, H., Ferrari, M. (2015) Principles of nanoparticle design for overcoming biological barriers to drug delivery. *Nat. Biotechnol. 33*, 941–951.

(16) Liu, J., Yu, M., Zhou, C., Zheng, J. (2013) Renal clearable inorganic nanoparticles: A new frontier of bionanotechnology. *Mater. Today. 12*, 477-486.

(17) Du, B., Jiang, X., Das, A., Zhou, Q., Yu, M., Jin, R., Zheng, J. (2017) Glomerular barrier behaves as an atomically precise bandpass filter in a sub-nanometre regime. *Nat. Nanotechnol. 11*, 1096-1102.

(18) Etheridge, M. L., Campbell, S., Erdman, A. G., Haynes, C. L., Wolf, S. M., McCullough, J. (2013) The big picture on nanomedicine: the state of investigational and approved nanomedicine products. *Nanomedicine 9*, 1–14.

(19) Yu, M., Zheng, J. (2015) Clearance Pathways and Tumor Targeting of Imaging Nanoparticles. *ACS Nano, 9*, 6655–6674.

(20) Arvizo, R. R. R., Bhattacharyya, S., Kudgus, R. A., Giri, K., Bhattacharya, R., Mukherjee, P. (2012) Intrinsic therapeutic applications of noble metal nanoparticles: past, present and future. *Chem. Soc. Rev. 41*, 2943–2970.

(21) Khlebtsov, N., Dykman, L. (2011) Biodistribution and toxicity of engineered gold nanoparticles: a review of in vitro and in vivo studies. *Chem. Soc. Rev. 40*, 1647–1671.

(22) Dreaden, E. C., Alkilany, A. M., Huang, X., Murphy, C. J., El-Sayed, M. A. (2012) The golden age: gold nanoparticles for biomedicine. *Chem. Soc. Rev. 41*, 2740–2779.

(23) Huang, H.-C., Barua, S., Sharma, G., Dey, S. K., Rege, K. (2011) Inorganic nanoparticles for cancer imaging and therapy. *J. Control. Release 155*, 344–357.

(24) Zarschler, K., Rocks, L., Licciardello, N., Boselli, L., Polo, E., Garcia, K. P., De Cola, L., Stephan, H., Dawson, K. A. (2016) Ultrasmall inorganic nanoparticles: state-of-the-art and perspectives for biomedical applications. *Nanomedicine Nanotechnology, Biol. Med. 12*, 1663–1701.

(25) Nguyen, K. T., Zhao, Y. (2015) Engineered Hybrid Nanoparticles for On-Demand Diagnostics and Therapeutics. *Acc. Chem. Res. 48*, 3016–3025.

(26) Dreaden, E. C., El-Sayed, M. A. (2012) Detecting and Destroying Cancer Cells in More than One Way with Noble Metals and Different Confinement Properties on the Nanoscale. *Acc. Chem. Res. 45*, 1854–1865.

(27) Bergamini, L., Voliani, V., Cappello, V., Nifosì, R., Corni, S. (2015) Non-linear optical response by functionalized gold nanospheres: identifying design principles to maximize the molecular photo-release. *Nanoscale 7*, 13345–13357.

(28) Dreaden, E. C., Mackey, M. A., Huang, X., Kang, B., El-Sayed, M. A. (2011) Beating cancer in multiple ways using nanogold. *Chem. Soc. Rev. 40*, 3391-3404.

(29) Ehlerding, E. B., Chen, F., Cai, W. (2015) Biodegradable and Renal Clearable Inorganic Nanoparticles. *Adv. Sci. 2*, 1500223.

(30) Sun, T., Zhang, Y. S., Pang, B., Hyun, D. C., Yang, M., Xia, Y. (2014) Engineered Nanoparticles for Drug Delivery in Cancer Therapy. *Angew. Chemie Int. Ed. 53*, 12320–12364.

(31) Ranalli, A., Santi, M., Capriotti, L., Voliani, V., Porciani, D., Beltram, F., Signore, G. (2017) Peptide-Based Stealth Nanoparticles for Targeted and pH-Triggered Delivery. *Bioconjug. Chem. 28*, 627–635.

(32) Santi, M., Maccari, G., Mereghetti, P., Voliani, V., Rocchiccioli, S., Ucciferri, N., Luin, S., Signore, G. (2017) Rational Design of a Transferrin-Binding Peptide Sequence Tailored to Targeted Nanoparticle Internalization. *Bioconjug. Chem. 28*, 471–480.

(33) Ning, X., Peng, C., Li, E. S., Xu, J., Vinluan, R. D., Yu, M., Zheng, J. (2017) Physiological stability and renal clearance of ultrasmall zwitterionic gold nanoparticles: Ligand length matters. *APL Mater. 5*, 053406.

(34) Moghimi, S. M., Hunter, A. C., Murray, J. C. (2001) Long-Circulating and Target-Specific Nanoparticles : Theory to Practice. *Pharmacol. Rev. 53*, 283–318.

(35) Soo Choi, H., Liu, W., Misra, P., Tanaka, E., Zimmer, J. P., Itty Ipe, B., Bawendi, M. G., Frangioni, J. V. (2007) Renal clearance of quantum dots. *Nat. Biotechnol. 25*, 1165–1170.

(36) Gong, L., Wang, Y., Liu, J. (2017) Bioapplications of renal-clearable luminescent metal nanoparticles. *Biomater. Sci. 5*, 1393–1406.

(37) Tam, J. M., Tam, J. O., Murthy, A., Ingram, D. R., Ma, L. L., Travis, K., Johnston, K. P., Sokolov, K. V. (2010) Controlled Assembly of Biodegradable Imaging and Therapeutic Applications. *ACS Nano 4*, 2178-2184.

(38) He, C.-F., Wang, S.-H., Yu, Y.-J., Shen, H.-Y., Zhao, Y., Gao, H.-L., Wang, H., Li, L.-L., Liu, H.-Y., He, C.-F., et al. (2016) Advances in biodegradable nanomaterials for photothermal therapy of cancer. *Cancer Biol. Med. 13*, 299–312.

16

(39) Deng, H., Dai, F., Ma, G., Zhang, X. (2015) Theranostic Gold Nanomicelles made from Biocompatible Comb-like Polymers for Thermochemotherapy and Multifunctional Imaging with Rapid Clearance. *Adv. Mater. 27*, 3645–3653.

(40) Rengan, A. K., Bukhari, A. B., Pradhan, A., Malhotra, R., Banerjee, R., Srivastava, R., De, A. (2015) In vivo analysis of biodegradable liposome gold nanoparticles as efficient agents for photothermal therapy of cancer. *Nano Lett. 15*, 842–848.

(41) Al Zaki, A., Joh, D., Cheng, Z., De Barros, A. L. B., Kao, G., Dorsey, J., Tsourkas, A. (2014) Gold-Loaded Polymeric Micelles for Computed Tomography-Guided Radiation Therapy Treatment and Radiosensitization. *ACS Nano 8*, 104–112.

(42) Tam, J. M., Tam, J. O., Murthy, A., Ingram, D. R., Ma, L. L., Travis, K., Johnston, K. P., Sokolov, K. V. (2010) Controlled assembly of biodegradable plasmonic nanoclusters for near-infrared imaging and therapeutic applications. *ACS Nano 4*, 2178–2184.

(43) Tam, J. M., Murthy, A. K., Ingram, D. R., Nguyen, R., Sokolov, K. V., Johnston, K. P. (2010) Kinetic assembly of near-IR-active gold nanoclusters using weakly adsorbing polymers to control the size. *Langmuir 26*, 8988–8999.

(44) Yoon, S. J., Murthy, A., Johnston, K. P., Sokolov, K. V., Emelianov, S. Y. (2012) Thermal stability of biodegradable plasmonic nanoclusters in photoacoustic imaging. *Opt. Express 20*, 29479.

(45) Murthy, A. K., Stover, R. J., Borwankar, A. U., Nie, G. D., Gourisankar, S., Truskett, T. M., Sokolov, K. V., Johnston, K. P. (2013) Equilibrium gold nanoclusters quenched with biodegradable polymers. *ACS Nano 7*, 239–251.

(46) Huang, P., Lin, J., Li, W., Rong, P., Wang, Z., Wang, S., Wang, X., Sun, X., Aronova, M., Niu, G., et al. (2013) Biodegradable gold nanovesicles with an ultrastrong plasmonic coupling effect for photoacoustic imaging and photothermal therapy. *Angew. Chemie - Int. Ed. 52*, 13958–13964.

(47) Deng, H., Zhong, Y., Du, M., Liu, Q., Fan, Z., Dai, F., Zhang, X. (2014) Theranostic self-assembly structure of gold nanoparticles for NIR photothermal therapy and X-Ray computed tomography imaging. *Theranostics 4*, 904–918.

(48) Yoon, S. J., Mallidi, S., Tam, J. M., Tam, J. O., Murthy, A., Johnston, K. P., Sokolov, K. V, Emelianov, S. Y. (2010) Utility of biodegradable plasmonic nanoclusters in photoacoustic imaging. *Opt. Lett. 35*, 3751–3753.

(49) Song, J., Yang, X., Jacobson, O., Huang, P., Sun, X., Lin, L., Yan, X., Niu, G., Ma, Q., Chen, X. (2015) Ultrasmall Gold Nanorod Vesicles with Enhanced Tumor Accumulation and Fast Excretion from the Body for Cancer Therapy. *Adv. Mater. 27*, 4910–4917.

(50) Yahia-Ammar, A., Sierra, D., Mérola, F., Hildebrandt, N., Le Guével, X. (2016) Self-Assembled Gold Nanoclusters for Bright Fluorescence Imaging and Enhanced Drug Delivery. *ACS Nano 10*, 2591–2599.

(51) Cheheltani, R., Ezzibdeh, R. M., Chhour, P., Pulaparthi, K., Kim, J., Jurcova, M., Hsu, J. C., Blundell, C., Litt, H. I., Ferrari, V. A., et al. (2016) Tunable, biodegradable gold nanoparticles as contrast agents for computed tomography and photoacoustic imaging. *Biomaterials 102*, 87–97.

(52) Feng, Q., Shen, Y., Fu, Y., Muroski, M. E., Zhang, P., Wang, Q., Xu, C., Lesniak, M. S., Li, G., Cheng, Y. (2017) Self-Assembly of Gold Nanoparticles Shows Microenvironment-Mediated Dynamic Switching and Enhanced Brain Tumor Targeting. *Theranostics 7*, 1875–1889.

(53) Wang, S., Chen, K. J., Wu, T. H., Wang, H., Lin, W. Y., Ohashi, M., Chiou, P. Y., Tseng, H. R. (2010) Photothermal effects of supramolecularly assembled gold nanoparticles for the targeted treatment of cancer cells. *Angew. Chemie - Int. Ed. 49*, 3777–3781.

(54) Jin, Y., Wang, J., Ke, H., Wang, S., Dai, Z. (2013) Graphene oxide modified PLA microcapsules containing gold nanoparticles for ultrasonic/CT bimodal imaging guided photothermal tumor therapy. *Biomaterials 34*, 4794–4802.

(55) Iodice, C., Cervadoro, A., Palange, A. L., Key, J., Aryal, S., Ramirez, M. R., Mattu, C., Ciardelli, G., O'Neill, B. E., Decuzzi, P. (2016) Enhancing photothermal cancer therapy by clustering gold nanoparticles into spherical polymeric nanoconstructs. *Opt. Lasers Eng. 76*, 74–81.

(56) Al Zaki, A., Hui, J. Z., Higbee, E., Tsourkas, A. (2015) Biodistribution, Clearance, and Toxicology of Polymeric Micelles Loaded with 0.9 or 5 nm Gold Nanoparticles. *J. Biomed. Nanotechnol. 11*, 1836–46.

(57) Mieszawska, A. J., Gianella, A., Cormode, D. P., Zhao, Y., Meijerink, A., Langer, R., Farokhzad, O. C., Fayad, Z. A., Mulder, W. J. M. (2012) Engineering of lipid-coated PLGA nanoparticles with a tunable payload of diagnostically active nanocrystals for medical imaging. *Chem. Commun. 48*, 5835-5837.

(58) Hembury, M., Chiappini, C., Bertazzo, S., Kalber, T. L., Drisko, G. L., Ogunlade, O., Walker-Samuel, S., Krishna, K. S., Jumeaux, C., Beard, P., et al. (2015) Gold–silica quantum rattles for multimodal imaging and therapy. *Proc. Natl. Acad. Sci. 112*, 1959–1964.

(59) Croissant, J. G., Zhang, D., Alsaiari, S., Lu, J., Deng, L., Tamanoi, F., AlMalik, A. M., Zink, J. I., Khashab, N. M. (2016) Protein-gold clusters-capped mesoporous silica nanoparticles for high drug loading, autonomous gemcitabine/doxorubicin co-delivery, and in-vivo tumor imaging. *J. Control. Release 229*, 183–191.

(60) Cassano, D., Santi, M., Cappello, V., Luin, S., Signore, G., Voliani, V. (2016) Biodegradable Passion Fruit-Like Nano-Architectures as Carriers for Cisplatin Prodrug. *Part. Part. Syst. Charact. 33*, 818–824.

(61) Avigo, C., Cassano, D., Kusmic, C., Voliani, V., Menichetti, L. (2017) Enhanced Photoacoustic Signal of Passion Fruit-Like Nanoarchitectures in a Biological Environment. *J. Phys. Chem. C 121*, 6955–6961.

(62) Rengan, A. K., Jagtap, M., De, A., Banerjee, R., Srivastava, R. (2014) Multifunctional gold coated thermo-sensitive liposomes for multimodal imaging and photo-thermal therapy of breast cancer cells. *Nanoscale 6*, 916–923.

(63) Carja, G., Grosu, E. F., Petrarean, C., Nichita, N. (2015) Self-assemblies of plasmonic gold/layered double hydroxides with highly efficient antiviral effect against the hepatitis B virus. *Nano Res. 8*, 3512–3523.

(64) Lai, X., Tan, L., Deng, X., Liu, J., Li, A., Liu, J., Hu, J. (2017) Coordinatively Self-Assembled Luminescent Gold Nanoparticles: Fluorescence Turn-On System for High-Efficiency Passive Tumor Imaging. *ACS Appl. Mater. Interfaces 9*, 5118–5127.

(65) Galper, M. W., Saung, M. T., Fuster, V., Roessl, E., Thran, A., Proksa, R., Fayad, Z. A., Cormode, D. P. (2012) Effect of computed tomography scanning parameters on gold nanoparticle and iodine contrast. *Invest. Radiol. 47*, 475–481.

(66) Pocoví-Martínez, S., Parreño-Romero, M., Agouram, S., Pérez-Prieto, J. (2011) Controlled UV-C light-induced fusion of thiol-passivated gold nanoparticles. *Langmuir 27*, 5234–41.

(67) Croissant, J. G., Fatieiev, Y., Khashab, N. M. (2017) Degradability and Clearance of Silicon, Organosilica, Silsesquioxane, Silica Mixed Oxide, and Mesoporous Silica Nanoparticles. *Adv. Mater. 29*, 1604634.

(68) Cassano, D., Rota Martir, D., Signore, G., Piazza, V., Voliani, V. (2015) Biodegradable hollow silica nanospheres containing gold nanoparticle arrays. *Chem. Commun. 51*, 9939–9941.

(69) Lammers, T., Subr, V., Ulbrich, K., Peschke, P., Huber, P. E., Hennink, W. E., Storm, G. (2009) Biomaterials Simultaneous delivery of doxorubicin and gemcitabine to tumors in vivo using prototypic polymeric drug carriers. *Biomaterials 30*, 3466–3475.

(70) Liu, D., Chen, Y., Feng, X., Deng, M., Xie, G., Wang, J., Zhang, L., Liu, Q., Yuan, P. (2014) Colloids and Surfaces B : Biointerfaces Micellar nanoparticles loaded with gemcitabine and doxorubicin showed synergistic effect. *Colloids Surfaces B Biointerfaces 113*, 158–168.

17

(71) Cassano, D., David, J., Luin, S., Voliani, V. (2017) Passion fruit-like nano-architectures: a general synthesis route. *Sci. Rep.* 7, 43795.

(72) D'Apice, R., Voliani, V. (2017) Increasing the metal loading in passion fruit-like nano-architectures. *Adv. Mater. Lett. 8,* 1156–1160.

(73) Schmid, G., Kreyling, W. G., Simon, U. (2017) Toxic effects and biodistribution of ultrasmall gold nanoparticles. *Arch. Toxicol. 91,* 3011–3037.

(74) Hainfeld, J. F., Dilmanian, F. A., Zhong, Z., Slatkin, D. N., Kalef-Ezra, J. A., Smilowitz, H. M. (2010) Gold nanoparticles enhance the radiation therapy of a murine squamous cell carcinoma. *Phys. Med. Biol. 55,* 3045–3059.

(75) Mesbahi, A. (2010) A review on gold nanoparticles radiosensitization effect in radiation therapy of cancer. *Reports Pract. Oncol. Radiother. J. Gt. Cancer Cent. Poznań Polish Soc. Radiat. Oncol. 15,* 176–180.

(76) Lusic, H., Grinstaff, M. W. (2013) X-ray-Computed Tomography Contrast Agents. *Chem. Rev. 113,* 1641–1666.

(77) Farhadi, A., Roxin, Å., Wilson, B. C., Zheng, G. (2015) Nano-enabled SERS reporting photosensitizers. *Theranostics 5,* 469–476.

(78) Torchilin, V. P. (2012) Multifunctional nanocarriers. *Adv. Drug Deliv. Rev. 64,* 302–315.

(79) Troutman, T. S., Barton, J. K., Romanowski, M. (2008) Biodegradable plasmon resonant nanoshells. *Adv. Mater. 20,* 2604–2608.

(80) Leung, S. J., Kachur, X. M., Bobnick, M. C., Romanowski, M. (2011) Wavelength-selective light-induced release from plasmon resonant liposomes. *Adv. Funct. Mater. 21,* 1113–1121.

(81) Leung, S. J., Romanowski, M. (2012) NIR-activated content release from plasmon resonant liposomes for probing single-cell responses. *ACS Nano 6,* 9383–9391.

(82) Eaton, M. A. W., Levy, L., Fontaine, O. M. A. (2015) Delivering nanomedicines to patients: A practical guide. *Nanomedicine Nanotechnology, Biol. Med. 11,* 983–992.

(83) Anchordoquy, T. J., Barenholz, Y., Boraschi, D., Chorny, M., Decuzzi, P., Dobrovolskaia, M. A., Farhangrazi, Z. S., Farrell, D., Gabizon, A., Ghandehari, H., et al. (2017) Mechanisms and Barriers in Cancer Nanomedicine: Addressing Challenges, Looking for Solutions. *ACS Nano 11,* 12–18.

(84) Barenholz, Y. (Chezy). (2012) Doxil® — The first FDA-approved nano-drug: Lessons learned. *J. Control. Release 160,* 117–134.

(85) Alkilany, A. M., Murphy, C. J. (2010) Toxicity and cellular uptake of gold nanoparticles: what we have learned so far? *J. Nanoparticle Res. 12,* 2313–2333.

(86) Dawidczyk, C. M., Kim, C., Park, J. H., Russell, L. M., Lee, K. H., Pomper, M. G., Searson, P. C. (2014) State-of-the-art in design rules for drug delivery platforms: Lessons learned from FDA-approved nanomedicines. *J. Control. Release 187,* 133–144.

(87) Sandoval, B. (MacDonald). (2009) Perspectives on FDA's Regulation of Nanotechnology: Emerging Challenges and Potential Solutions. *Compr. Rev. Food Sci. Food Saf. 8,* 375–393.

(88) Anselmo, A. C., Mitragotri, S. (2016) Nanoparticles in the clinic. *Bioeng. Transl. Med. 1,* 10–29.

(89) Desai, N. (2012) Challenges in Development of Nanoparticle-Based Therapeutics. *AAPS J. 14,* 282–295.

(90) Sainz, V., Conniot, J., Matos, A. I., Peres, C., Zupančič, E., Moura, L., Silva, L. C., Florindo, H. F., Gaspar, R. S. (2015) Regulatory aspects on nanomedicines. *Biochem. Biophys. Res. Commun. 468,* 504–510.

(91) Schellekens, H., Stegemann, S., Weinstein, V., de Vlieger, J. S. B., Flühmann, B., Mühlebach, S., Gaspar, R., Shah, V. P., Crommelin, D. J. A. (2014) How to Regulate Nonbiological Complex Drugs (NBCD) and Their Follow-on Versions: Points to Consider. *AAPS J. 16,* 15–21.

(92) Voliani, V., Gemmi, M., Francés-Soriano, L., González-Béjar, M., Pérez-Prieto, J. (2014) Texture and Phase Recognition Analysis of β-NaYF4 Nanocrystals. *J. Phys. Chem. C 118,* 11404–11408.

(93) Malinoski, F. J. (2014) The nanomedicines alliance: an industry perspective on nanomedicines. *Nanomedicine Nanotechnology, Biol. Med. 10,* 1819–1820.

18

TOC

Best Excretion
Poor Theranostics

<5nm

Best Theranostics
Accumulation

>20nm

Ultrasmall-in-nano

Theranostics + Excretion

19